ELECTRON CLOUD IN THE WIGGLERS OF THE POSITRON DAMPING RING OF THE INTERNATIONAL LINEAR COLLIDER*

L. Wang#, SLAC, CA 94025, U.S.A.
F. Zimmermann, CERN, Geneva, Switzerland

Abstract

The ILC positron damping ring comprises hundreds of meters of wiggler sections, where many more photons than in the arcs are emitted, and with the smallest beam-pipe aperture of the ring. A significant electron-cloud density can therefore be accumulated via photo-emission and via beam-induced multipacting. In field-free regions the electron-cloud build up may be suppressed by adding weak solenoid fields, but the electron cloud remaining in the wigglers as well as in the arc dipole magnets can still drive single-bunch and multi-bunch beam instabilities. This paper studies the electron-cloud formation in an ILC wiggler section for various scenarios, as well as its character, and possible mitigation schemes.

INTRODUCTION

The updated ILC baseline design foresees a single positron damping ring. Table 1 lists its key parameters.

Table 1: Parameters of the 6.7-km ILC damping ring

Description	Value
Beam energy	5.0 GeV
Circumference	6695 km
Harmonic number	14516
RF frequency	650 MHz
Tunes	52.28/47.40
Momentum compaction	0.40×10^{-3}
Number of bunches	2767~5782
Bunch intensity	$0.97\text{~}2.02\times10^{10}$
Emittance at injection	5.0×10^{-10}m
Average betatron function	22.5m

Compared with the two B-factories, the bunch intensity is lower. However, the bunch spacing is shorter as well, and, together with the smaller aperture of the ILC beam pipe, the net result should be a larger electron cloud in general. The electron cloud in the field free regions can be suppressed by weak solenoidal fields, as were successfully applied at both B-factories. The electron cloud build up in a dipole magnet is well understood by both experiments and simulations for the CERN SPS [1, 2]. The electron-cloud in the DAFNE wiggler is suspected to be the cause of a positron-beam instability observed following modifications to the wiggler field [3]. The electron cloud in the ILC damping ring will be dominated by electrons present in magnets, with the hundreds of meters of wiggler sections playing an important role. A better understanding of the electron cloud in the wiggler is a crucial milestone towards an efficient suppression. This paper studies the electron-cloud build up and the electron distribution in an ILC wiggler by means of simulations [4]. The effects of the magnetic field, beam filling pattern, possible remedies, etc. are investigated in detail. For some earlier simulations of electron clouds in wigglers see [3].

*Work supported by the U.S. Department of Energy under contract DE-AC03-76SF00515
electric address: wanglf@slac.stanford.edu

SIMULATION MODEL

According to the Halbach formulae [5] the magnetic field of the wiggler can be expressed as

$$
\begin{aligned}
B_x &= \frac{k_x}{k_y} B_0 \sinh(k_x x)\sinh(k_y y)\cos(kz) \\
B_y &= B_0 \cosh(k_x x)\cosh(k_y y)\cos(kz), \qquad (1) \\
B_z &= -\frac{k}{k_y} B_0 \cosh(k_x x)\sin(k_y y)\sin(kz)
\end{aligned}
$$

where $k_{x,y}$ and k satisfy

$$k_{x,n}^2 + k_{y.n}^2 = (nk)^2 = (n2\pi/\lambda)^2 . \qquad (2)$$

The total field is obtained by summing all components,

$$\vec{B} = \sum_{n=1,3,\ldots,N} B_n \vec{f}_n(k_{x,n}, k_{x,n}, nk, x, y, z) , \qquad (3)$$

$$k_{x,n}^2 + k_{y,n}^2 = (nk)^2 \ . \qquad (4)$$

Here we consider only the fundamental component n=1, and also assume $k_{x,1}$=0, which is a good approximation at small |x| where multipacting occurs. When $k_{x,1}$=0, B_y and B_z are independent of the horizontal position, and B_x vanishes. In this study we take a peak field of 1.68 *T* with a period of 0.40 *m*. For the maximum secondary emission yield (SEY) we choose the typical value 1.4[1].

RESULTS

Mirror field trapping

The vertical field B_y has a minimum at the vertical center y=0, so that the magnetic field resembles a mirror field i.e. one which may trap electrons via the mirror-field trapping mechanism. Figure 1 displays the orbit of a single electron generated by ionization near the beam. Either because it is reflected by the mirror field, or due to the attraction by the beam field, at y=-5mm this electron inverts its direction of motion, starts moving upwards, and finally hits the top surface of the beam pipe. But the simulated build-up pattern and electron distribution indicate the absence of “deep” trapping. We attribute this to the small variation of B_y near the vertical center (cosh function). Another possible reason is that the largest momentum component electrons near the wiggler poles acquire in the beam field is the vertical one, since their gyration period is shorter than the bunch passage.

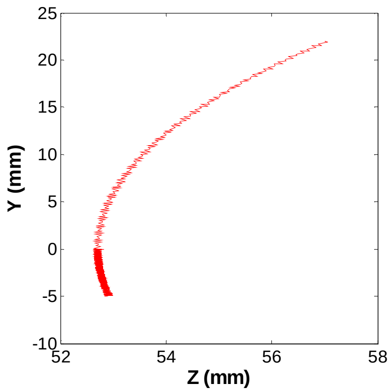

Figure 1: Orbit of a single electron in the wiggler. This electron is generated near the chamber center by gas ionization. It first moves down, and then upwards.

Electron-cloud distribution

The three-dimensional (3-D) wiggler field (1) translates into a 3-D electron distribution, which is illustrated in Fig.2, presenting the stereographic projections onto the **xy** and **xz** planes. The transverse distribution (**xy** plane) is similar to that in a uniform dipole magnet: There are two multipacting strips near the horizontal center [1,2,4]. In the **xz** plane, a clear dependence on z is visible. The electron density is minimum near the region where B_y=0 (cos(kz)=0), i.e. halfway between two successive magnet poles. These minima are easily explained by the magnetic field distribution of Fig. 3: The regions of lowest electron density coincide with those where the longitudinal field component is largest. The latter can suppress electron multipacting just like a solenoid field.

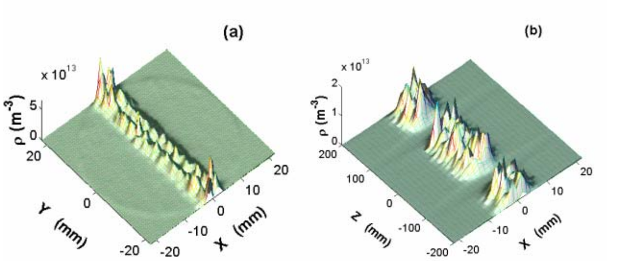

Figure 2: Electron distribution in a wiggler: Transverse plane (a) and horizontal-longitudinal plane (b).

Filling pattern effect

The number of ILC bunches varies from about 3000 to 6000, while the total beam current is kept constant. A number of beam injection modes result in different beam patterns. We study two particular beam patterns: 2767 bunches and 5782 bunches. The 2767 beam fill pattern consists of 125 bunch trains with 22 or 23 bunches each. The 5782 beam fill pattern contains 118 bunch trains with 49 bunches per train. The gap between successive bunch trains is 38 *ns* and 43 *ns* for the 2767 and 5782 bunches fill patterns, respectively. The bunch spacing is 6 ns and 3 ns for the fill pattern with 2767 and 5782 bunches, respectively. The total beam current is the same for the two filling patterns.

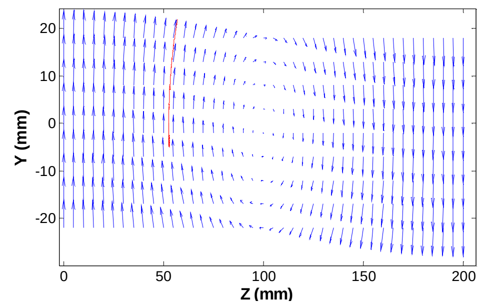

Figure 3: Magnetic field in the vertical-longitudinal plane of a wiggler with 0.4-m period. The red line represents the electron trajectory of Fig. 1.

Figure 4 compares the build up of the electron cloud in the case of a single long bunch train with that for a multi-train pattern of 2767 bunches. It is evident that the multi-train filling pattern reduces the electron cloud density by a factor of 5. In Fig. 5, the build up for two different multi-train patterns is compared. The low-Q beam pattern (5782 bunches) results in a 10 times lower electron density.

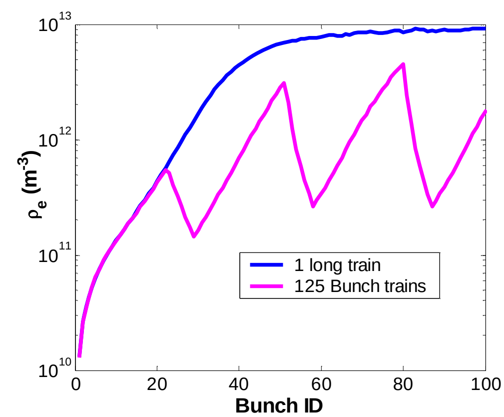

Figure 4: Electron build-up for a single long bunch train and for a multi-train, with 2767 bunches in total.

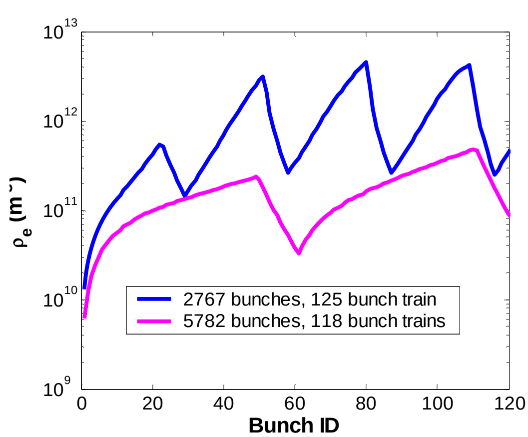

Figure 5: Electron cloud build-up for different multi-train filling patterns: 125-bunch trains and 118-bunch trains.

Comparison with dipole magnet

Figure 6 shows the transverse electron distribution in a uniform 0.19-T arc dipole field. As for the wiggler two strips are observed, but these two strips are further apart than for the (stronger) wiggler field. Preliminary studies show that the peak electron density in the dipole magnet is larger than that in a wiggler by a factor of 2.7 (Fig. 7). Probably this is due to the variation of the field with longitudinal position and the absence of multipacting in the region between successive wiggler poles.

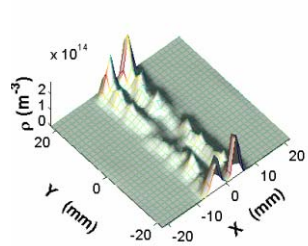

Figure 6: Transverse electron distribution in a uniform dipole magnet with 0.19-T field.

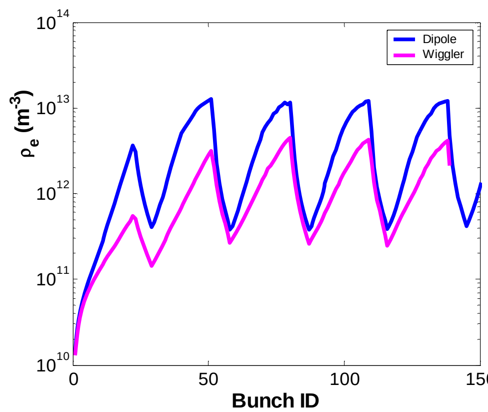

Figure 7: Electron build up in a dipole and in a wiggler, for a beam of 2767 bunches and 125 bunch trains.

Ionization electrons and wiggler period

In all the above studies (except for Fig.1), the primary electrons were assumed to be photo-electrons. If the electrons are generated by gas ionization instead, the electron build up usually takes a longer time, until finally about the same saturation level is reached (Fig. 8). This is because the maximum electron cloud density is always limited by the electron space-charge field. The electron distribution in the longitudinal direction is similar, but horizontally it differs: There is only one strip of electrons near x=0 for the case of gas-ionization, as is illustrated in Fig. 9, in contrast to the two strips for photo-electrons, in Fig. 2. This difference can be explained by the strong wiggler field which confines the electrons and their secondaries to their initial horizontal position. In the case of gas ionization no primary electrons are generated in the region of the two strips where multipacting would otherwise be strongest.

Since the electron cloud varies with the longitudinal position (Fig. 2), we may expect a dependence also on the wiggler period. Simulations show that a wiggler field of 0.2-m period reduces the electron density by 30% compared with a 0.4-m period.

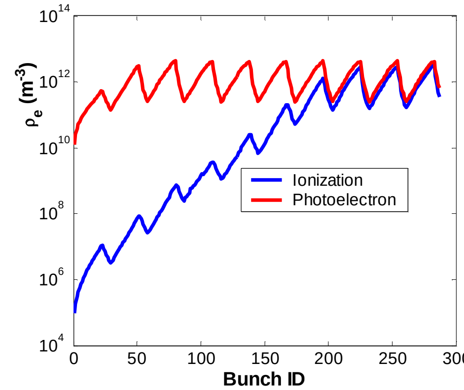

Figure 8: Build up of electron cloud with either photo-electrons or gas-ionization as primary electron source, for 1 nTorr vacuum pressure, and 2767 beam filling pattern.

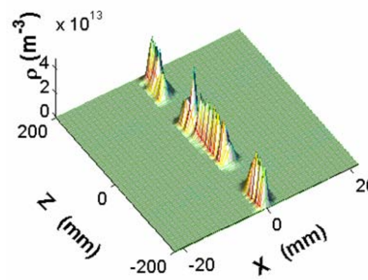

Figure 9: Distribution of the electron cloud in the longitudinal-horizontal plane for gas ionization.

Other remedies

Solenoids do not work for the wiggler. A clearing electrode [6] or a triangular grooved chamber [7] can easily suppress the electron multipacting. Recently an electron-cloud clearing electrode was successfully tested at the CERN PS [8]. Further tests in dipoles and wigglers are planned at KEKB and CESR. Surface coating significantly reduces the SEY down to about 1.0 [9]. A triangular grooved chamber in a PEP-II dipole should reduce the SEY of a TiN-coated surface to below 0.7 [10].

REFERENCES

[1] J.M. Jimenez et al, CERN-LHC-Project-Report-632 (2003).
[2] D. Schulte et al, Proc.PAC2005 Knoxville (2005) 1371
[3] F. Zimmermann, D. Schulte, R. Cimino, C.Vaccarezza, M. Zobov, R. Wanzenberg, CLIC Note 650, EUROTEV-REPORT 2006-002-1.
[4] L. Wang, H. Fukuma, K. Ohmi, S. Kurokawa, K. Oide, and F. Zimmermann, Physical Review Special Topics- Accelerators and Beams, 5, 124402 (2002).
[5] K. Halbach, Nucl.Inst. and meth. Vol 78 pp265, 1970
[6] L. Wang, et. al., Proceedings of EPAC06, 1489-149.
[7] L. Wang, T. Raubenheimer and G. Stupakov, Nucl. Instr. and Meth. A, 571 (2007) 588–598.
[8] F. Caspers, T. Kroyer, E. Mahner, et al, priv. comm.
[9] http://chep.knu.ac.kr/ecloud07/
[10] L. Wang, et. al., these proceedings.

